

# Numerical simulation of supercell tornadogenesis associated with Typhoon Shanshan (2006)

Wataru Mashiko

Meteorological Research Institute, JMA, 1-1 Nagamine, Tsukuba, Ibaraki 305-0052, Japan  
(E-mail : wmashiko@mri-jma.go.jp)

## 1. Introduction

On 17 September 2006, three tornados hit the Miyazaki Prefecture in western Japan during the passage of the rainband which accompanied Typhoon Shanshan (2006). The tornado which hit Nobeoka city caused most severe damage, and it was assessed with F-2 scale. In order to investigate the environmental field, tornadic parent storm and tornado itself, the numerical simulations with high resolution were conducted (Mashiko 2007) using the nonhydrostatic model developed by Japan Meteorological Agency (Saito et al. 2006). The environmental field around which the tornado occurred was characterized by modest CAPE ( $\sim 1000 \text{ J kg}^{-1}$ ) and strong low-level wind shear with veering. Some simulated convective cells in the outer rainband exhibited characteristics of a mini-supercell storm. They displayed differences from typical supercell storm on the Midwest in the U. S. with respect to the following points: 1) horizontal scale of the mesocyclone was smaller, 2) vertical vorticity was confined to lower levels (less than 5 km above ground level), and 3) near-surface temperature gradient around the gust front was slight ( $\sim 1 \text{ K}$ ). When the mini supercell storm approached the coast of Nobeoka city, a tornado was successfully reproduced using the model with a horizontal grid spacing of 50 m. The simulated tornado with a diameter of about 500 m has about  $1.0 \text{ s}^{-1}$  vertical vorticity near the ground. Obviously, it is difficult to say that one is simulating the exact observed tornado at a given time and location. However, the simulation should be able to reproduce the representative type of the storms that would actually occur on this environmental field. Note that this simulation includes full-physics processes. Therefore, it is unlike the other previous studies employing free-slip surface condition. In this study, we will focus on the generation process of the tornado in the mini-supercell storm.

## 2. Evolution of Low-level mesocyclone prior to tornadogenesis

Figure 1 shows the time-height cross section of maximum vertical vorticity and minimum pressure perturbation around the low-level mesocyclone center. The low-level mesocyclone in the mini-supercell storm is descending and intensifying with time. It subsequently connects to the tornado occurrence around 14:27 Local Time. The vertical vorticity reaches  $1.0 \text{ s}^{-1}$  near surface.

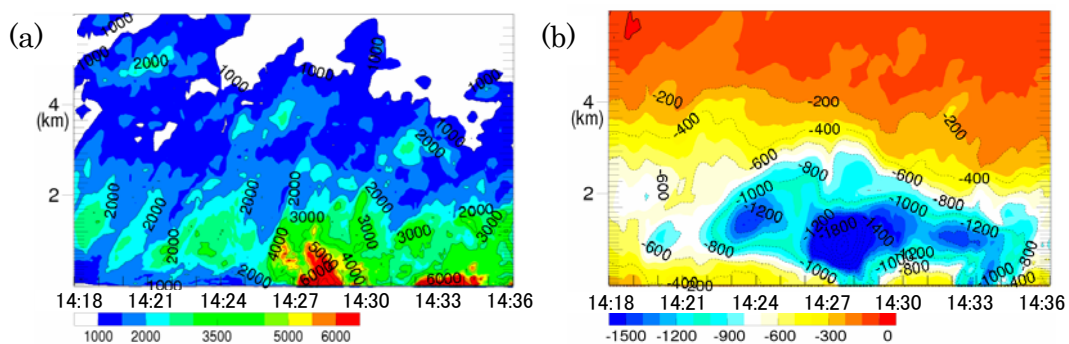


Fig. 1. Time-height cross section of (a) maximum vertical vorticity ( $\times 10^{-4} \text{ s}^{-1}$ ), and (b) minimum pressure perturbation (Pa). Each value is calculated within a 2.5 km radius of mesocyclone center determined as the location of maximum vorticity on the 1km square averaged field at a height of 1 km.

### 3. Generation process of the tornado in the mini-supercell storm

As the low-level mesocyclone intensified, hook-shaped hydrometeors became prominent (Fig. 2a). Rear-flank downdraft (RFD) associated with the hook-shaped hydrometeors was gradually intensifying and wrapping around the near-surface mesocyclone center (Fig. 2b). The tornado was generated between the left-front side of the RFD and the horseshoe-shaped updraft along the gust front (Figs. 2b and 2c). Actually, backward trajectories originating from the tornado show that about half of parcels traveled along the RFD (Fig. 3). When the RFD descended to the ground, it spread out and wrapped around the low-level mesocyclone. As it hit the leading edge of the rear-flank gust front, it could produce localized strong convergence and spin up the tornado.

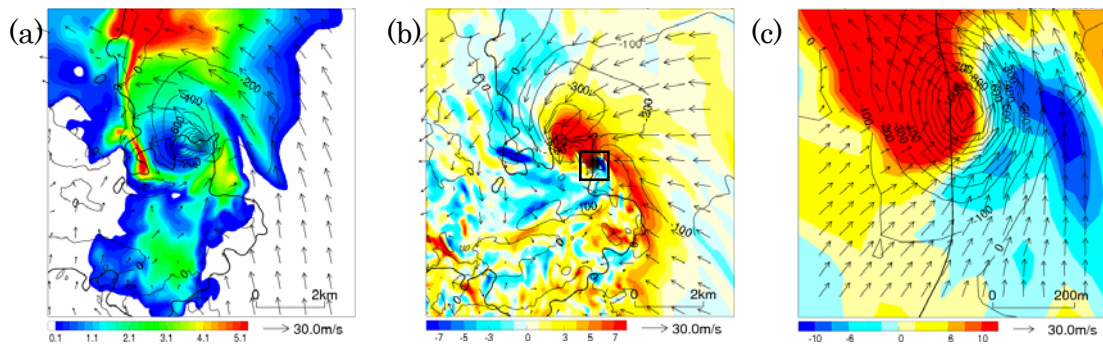


Fig. 2. Horizontal distribution of (a) hydrometeors ( $\text{g kg}^{-1}$ ) at height of 1 km, (b) vertical motion ( $\text{m s}^{-1}$ ) at a height of 250 m at 14:27 Local Time. (c) Enlarged display of the rectangle area in (b). Vectors depict storm-relative winds. Contours indicate pressure perturbation (Pa).

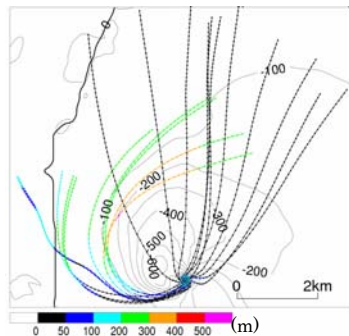


Fig. 3. Projection of the three-dimensional backward trajectories. Parcels were started from the tornado location at a height of 150 m and integrated from 14:27 to 14:22. Colors of the trajectory path indicate the parcel height. Solid contours indicate the pressure perturbation (Pa) at origin time (14:27).

### 4. Sensitivity to the effect of evaporation cooling and precipitation loading

Sensitivity experiments were conducted to confirm the effect of evaporation cooling and precipitation loading on the RFD and tornadogenesis. In the experiment with no evaporation cooling, the behavior of the RFD and tornadogenesis were almost same as those of the control experiment. The evaporation cooling worked little unlike the typical supercell storm on the Midwest in the U. S. In the meanwhile, the RFD didn't wrap around the low-level mesocyclone and the tornado was not generated on the experiment in which the precipitation loading was neglected on the buoyancy term. Thus, the precipitation loading associated with the hook-shaped hydrometeors plays a key role in the RFD and subsequent tornadogenesis.

### REFERENCES

- Mashiko, W. 2007: Numerical simulation of tornado-producing supercell storm and tornado associated with Typhoon Shanshan (2006).
- Saito, K., T. Fujita, Y. Yamada, J. Ishida, Y. Kumagai, K. Aranami, S. Ohmori, R. Nagasawa, S. Kumagai, C. Muroi, T. Kato, H. Eito, and Y. Yamazaki, 2006: The operational JMA nonhydrostatic mesoscale model. *Mon. Wea. Rev.*, 134, 1266-1298.